

Power Flow Control of a Doubly-Fed Induction Machine Coupled to a Flywheel*

Carles Batlle^{1,2}, Arnau Dòria-Cerezo² and Romeo Ortega³

¹Department of Applied Mathematics IV, UPC, EPSEVG, Avenue V. Balaguer s/n, 08800 Vilanova i la Geltrú, Spain;

²Institute of Industrial and Control Engineering, UPC, Avenue Diagonal 647, 08028 Barcelona, Spain;

³Laboratory des Signaux et Systèmes, CNRS-SUPELEC, Gif-sur-Yvette 91192, France

We consider a doubly-fed induction machine – controlled through the rotor voltage and connected to a variable local load – that acts as an energy-switching device between a local prime mover (a flywheel) and the electrical power network. The control objective is to optimally regulate the power flow, and this is achieved by commuting between different steady-state regimes. We first show that the zero dynamics of the system is only marginally stable; thus, complicating its control via feedback linearization. Instead, we apply the energy-based Interconnection and Damping Assignment Passivity-Based Control technique that does not require stable invertibility. It is shown that the partial differential equation that appears in this method can be circumvented by fixing the desired closed-loop total energy and adding new terms to the interconnection structure. Furthermore, to obtain a globally defined control law we introduce a state-dependent damping term that has the nice interpretation of effectively decoupling the electrical and mechanical parts of the system. This results in a globally convergent controller parameterized by two degrees of freedom, which can be used to implement the power management policy.

*This work has been done in the context of the European sponsored project Geoplex with reference code IST-2001-34166. Further information is available at <http://www.geoplex.cc>. The work of C.B. has been partially done with the support of the Spanish project Mocoshev, DPI2002-03279. The work of A.D.-C. was (partially) supported through a European Community Marie Curie Fellowship in the framework of the European Control Training Site.

E-mail:

Correspondence to: Romeo Ortega

The controller is simulated and shown to work satisfactorily for various realistic load changes.

Keywords: Doubly-Fed Induction Machine; Passivity-based Control; Port-Hamiltonian Models; Power Flow Control

1. Introduction

Doubly-fed induction machines (DFIMs) have been proposed in the literature, among other applications, for high-performance storage systems [2], wind-turbine generators [11,13] or hybrid engines [3]. The attractiveness of the DFIM stems primarily from its ability to handle large-speed variations around the synchronous speed (see Ref. [15] for an extended literature survey and discussion). In this paper we are interested in the application of DFIM as part of an autonomous energy-switching system that regulates the energy flow between a local prime mover (a flywheel) and the electrical power network, in order to satisfy the demand of a time-varying electrical load.

Most DFIM controllers proposed in the literature are based on vector-control and decoupling [8]. Along these lines, an output feedback algorithm for power control with rigorous stability and robustness results is presented in Ref. [15]. In this paper we propose an

Received January 31, 2005; Accepted May 30, 2005.

Recommended by A. Artolfi and A.J. van der Schaft.

alternative viewpoint and use the energy-based principles of passivity and control as interconnection [4,7,10,16]. More specifically, we prove that the Interconnection and Damping Assignment Passivity-Based Control (IDA-PBC) technique proposed in Ref. [10] can be easily applied to regulate the dynamic operation of this bidirectional power flow system.

The paper is organized as follows. In Section 2 we introduce the architecture of the system to be controlled and derive its model. Since IDA-PBC concerns the stabilization of equilibrium points, we use the well-known Blondel–Park synchronous dq -coordinates¹ to write the equations in the required form. Then, to render more transparent the application of IDA-PBC, we give the Port-Controlled Hamiltonian (PCH) version of the model. Section 3 discusses the zero dynamics of interest for the kind of task we are trying to solve and show it to be only marginally stable – hampering the application of control schemes relying on stable invertibility, such as feedback linearization or the Standard PBC reported previously [9]. The power management scheme consists of the assignment of suitable fixed points and is introduced in Section 4. The main result of the paper, presented in Section 5, is the proof that IDA-PBC renders each of the desired equilibria globally stable. We start with the solution of the partial differential equation (PDE) that arises in IDA-PBC by direct assignment of the desired energy function and modification of the interconnection structure. Unfortunately, the resulting control law contains a singularity; hence, it is not globally defined. To remove this singularity we introduce a state-dependent damping that, in the spirit of the nested-loop PBC configuration of Chapter 8 in Ref. [9], has the nice interpretation of effectively decoupling the electrical and mechanical parts of the system and Section 6 presents the results of several simulations. Conclusions are stated in Section 7.

Notation. Throughout the paper we use standard notation of electromechanical systems, with λ , v , i , τ , θ , ω denoting flux, voltage, current, torque, angular position and velocity, respectively; while R , L , J_m , B are used for resistance, inductance, inertia and friction parameters, respectively. Self-explanatory sub-indices are introduced also for the signals and parameters of the different subsystems. Finally, to underscore the port interconnection structure of the overall system we usually present the variables in power conjugated couples, i.e. port variables whose product has units of power.

¹In these coordinates the natural steady-state orbits are transformed into fixed points.

2. The System and its Mathematical Model

Figure 1 shows a DFIM, controlled through the rotor windings port (v_r, i_r) , coupled with an energy-storing flywheel with port variables (τ_e, ω) , an electrical network modelled by an ideal AC voltage source with port variables (v_n, i_n) , and a generic electrical load represented by its impedance Z_l . The main objective of the system is to supply the required power to the load with a high network power factor. Depending on the load demands, the DFIM acts as an energy-switching device between the flywheel and the electrical power network. The control problem is to optimally regulate the power flow. We will show below that this is achieved by commuting between different steady-state regimes.

Network equations are given by Kirchoff laws

$$i_l = i_n - i_s, \quad v_n = v_s. \quad (1)$$

Figure 2 shows a scheme of a doubly-fed, three-phase induction machine. It contains six energy storage elements with their associated dissipations and six

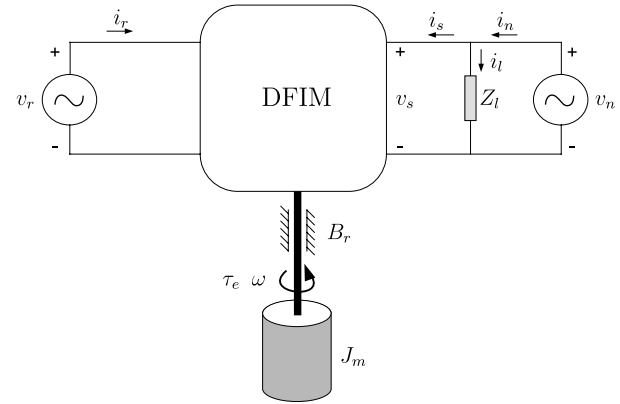


Fig. 1. Doubly-fed induction machine, flywheel, power network and load.

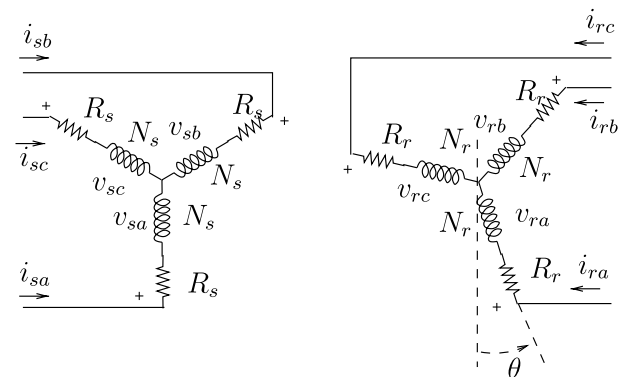


Fig. 2. Basic scheme of the doubly-fed induction machine.

ports (the three stator and the three rotor voltages and currents).

From the original three phase electrical variables y_{abc} (currents, voltages or magnetic fluxes) we compute transformed variables by means of

$$y = Ty_{abc},$$

where

$$T = \begin{pmatrix} \frac{\sqrt{2}}{\sqrt{3}} & -\frac{1}{\sqrt{6}} & -\frac{1}{\sqrt{6}} \\ 0 & \frac{1}{\sqrt{2}} & -\frac{1}{\sqrt{2}} \\ \frac{1}{\sqrt{3}} & \frac{1}{\sqrt{3}} & \frac{1}{\sqrt{3}} \end{pmatrix}.$$

Note that, since $T^T = T^{-1}$, this is a power-preserving transformation:

$$\langle i, v \rangle = \langle i_{abc}, v_{abc} \rangle.$$

As it is common, from now on we will work only with the first two components (the dq components) of any electrical quantity and neglect the third one (the homopolar component, which is zero for any balanced set and which, in any case, is decoupled from the remaining dynamical equations).

The electrical equations of motion in the original windings frame for the dq variables, neglecting nonlinear effects and non-sinusoidal magnetomotive force distribution, take the form [6],

$$\dot{\lambda}_s + R_s I_2 i_s = v_s \quad (2)$$

$$\dot{\lambda}_r + R_r I_2 i_r = v_r \quad (3)$$

where $\lambda_s, \lambda_r, i_s, i_r \in \mathbb{R}^2$ and

$$I_2 = \begin{bmatrix} 1 & 0 \\ 0 & 1 \end{bmatrix},$$

while the mechanical equations are given by (we assume without loss-of-generality a 2-poles machine)

$$\begin{aligned} J_m \dot{\omega} &= L_{sr} i_s^T J_2 i_r - B_r \omega \\ \dot{\theta} &= \omega \end{aligned} \quad (4)$$

where $\theta \in \mathbb{R}$, $J_m > 0$, $B_r \geq 0$, $L_{sr} > 0$ and

$$J_2 = \begin{bmatrix} 0 & -1 \\ 1 & 0 \end{bmatrix}.$$

Linking fluxes and currents are related by

$$\lambda = L(\theta) i$$

where

$$\lambda = \begin{bmatrix} \lambda_s \\ \lambda_r \end{bmatrix}, \quad i = \begin{bmatrix} i_s \\ i_r \end{bmatrix}, \quad L(\theta) = \begin{bmatrix} L_s I_2 & L_{sr} e^{J_2 \theta} \\ L_{sr} e^{-J_2 \theta} & L_r I_2 \end{bmatrix},$$

with $L_s, L_r > 0$ and $L_s L_r > L_{sr}^2$. Putting together (2) and (3) we get

$$\dot{\lambda} + \mathcal{R} i = V,$$

where

$$V = \begin{bmatrix} v_s \\ v_r \end{bmatrix}, \quad \mathcal{R} = \begin{bmatrix} R_s I_2 & O_2 \\ O_2 & R_r I_2 \end{bmatrix}, \quad O_2 = \begin{bmatrix} 0 & 0 \\ 0 & 0 \end{bmatrix}.$$

The steady-state for the equations above are periodic orbits that can be transformed into equilibrium points by means of the well-known Blondel–Park transformation [6]. This standard procedure also eliminates the dependence of the equations on θ , and consists in defining new variables f^r via

$$f = K(\theta, \delta) f^r$$

$$K(\theta, \delta) = \begin{bmatrix} e^{J_2 \delta} & O_2 \\ O_2 & e^{J_2(\delta - \theta)} \end{bmatrix}$$

where δ is an arbitrary function of time that, for convenience, we select as

$$\dot{\delta} = \omega_s,$$

with ω_s the line frequency, which is assumed constant.²

Applying this transformation to all the electrical variables, one gets

$$\mathcal{L} \dot{x} + [\Omega(\omega) \mathcal{L} + \mathcal{R}] x = M_1 u + M_2 v_s^r, \quad (5)$$

where

$$x = \begin{bmatrix} i_s^r \\ i_r^r \end{bmatrix}, \quad u = v_r^r, \quad v_s^r = \begin{bmatrix} V_0 \\ 0 \end{bmatrix}$$

$$\mathcal{L} = K^{-1}(\theta, \delta) L(\theta) K(\theta, \delta) = \begin{bmatrix} L_s I_2 & L_{sr} I_2 \\ L_{sr} I_2 & L_r I_2 \end{bmatrix}$$

$$\Omega(\omega) \mathcal{L} = \begin{bmatrix} \omega_s L_s J_2 & \omega_s L_{sr} J_2 \\ (\omega_s - \omega) L_{sr} J_2 & (\omega_s - \omega) L_r J_2 \end{bmatrix}$$

$$M_1 = \begin{bmatrix} O_2 \\ I_2 \end{bmatrix}, \quad M_2 = \begin{bmatrix} I_2 \\ O_2 \end{bmatrix}$$

with $V_0 > 0$ the constant voltage set by the power network.

The overall system consists of the fourth-order electrical dynamics (5) together with the scalar

²This is the so-called synchronous reference frame. Note the simple form of v_s^r in this frame.

mechanical dynamics (4). The control input is the two-dimensional rotor voltage u , and v_s^r is viewed as a constant disturbance.³

As discussed in Ref. [16] (and references therein) a large class of physical systems of interest in control applications can be modelled in the general form of PCH systems⁴

$$\dot{z} = [\mathcal{J}(z) - \mathcal{R}(z)](\nabla H)^\top + g(z)u,$$

where z is the state, $H(z)$ is the Hamiltonian of the system (representing its energy), $\mathcal{J}(z) = -\mathcal{J}^\top(z)$ is the interconnection matrix and $\mathcal{R}(z) = \mathcal{R}^\top(z) \geq 0$ the dissipation matrix. It is easy to see that PCH systems are passive with $(u, g^\top(z)(\nabla H)^\top)$ as port variables, and the total energy as storage function. Before closing this section we derive the PCH model of the system, a step which is instrumental for the application of the IDA-PBC methodology.

To cast our system into this framework it is convenient to select as state coordinates the natural electromechanical Hamiltonian variables, fluxes (λ) and (angular) momentum ($J_m\omega$), that is

$$z = \begin{bmatrix} z_e \\ z_m \end{bmatrix} = \begin{bmatrix} \lambda \\ J_m\omega \end{bmatrix},$$

where, for convenience, we have introduced a natural partition between electrical ($z_e \in \mathbb{R}^4$) and mechanical ($z_m \in \mathbb{R}$) coordinates. The equations of our system can be written as [12]

$$\dot{z} = [\mathcal{J}(z) - \mathcal{R}](\nabla H)^\top + B_1 v_r + B_2 v_s \quad (6)$$

with total energy

$$H(z) = \frac{1}{2} z_e^\top \mathcal{L}^{-1} z_e + \frac{1}{2J_m} z_m^2,$$

interconnection and dissipation matrices given, respectively, by

$$\mathcal{J}(z) = \begin{bmatrix} -\omega_s L_s J_2 & -\omega_s L_{sr} J_2 & O_{2 \times 1} \\ -\omega_s L_{sr} J_2 & -(\omega_s - \omega) L_r J_2 & L_{sr} J_2 i_s \\ O_{1 \times 2} & L_{sr} i_s^\top J_2 & 0 \end{bmatrix},$$

$$\mathcal{R} = \begin{bmatrix} R_s I_2 & O_2 & O_{2 \times 1} \\ O_2 & R_r I_2 & O_{2 \times 1} \\ O_{1 \times 2} & O_{1 \times 2} & B_r \end{bmatrix},$$

³To simplify the notation, in the sequel we will omit the super-index $(\cdot)^r$.

⁴To distinguish between energy-conserving and dissipating systems the latter are sometimes called PCHD systems.

and

$$B_1 = \begin{bmatrix} O_2 \\ I_2 \\ O_{2 \times 1} \end{bmatrix}, \quad B_2 = \begin{bmatrix} I_2 \\ O_2 \\ O_{2 \times 1} \end{bmatrix}.$$

Note that the gradient of the Hamiltonian yields the original, Lagrangian (or co-energy) variables:

$$(\nabla H)^\top = \begin{bmatrix} \mathcal{L}^{-1} z_e \\ \frac{1}{J_m} z_m \end{bmatrix} = \begin{bmatrix} x \\ \omega \end{bmatrix}$$

3. Zero Dynamics

As explained in Section 4, the power flow control for our system is based on the selection of appropriate constant values of the stator current. Thus, we study the zero dynamics of the system, taking i_s as output:

$$y = Cx$$

where $C = [I_2 \quad O_2]$. One easily gets

$$\dot{y} = C\mathcal{L}^{-1}[-(\Omega(\omega)\mathcal{L} + \mathcal{R})x + M_1 u + M_2 v_s].$$

We consider a constant desired output of the form $y^* = i_s^*$. Then $\dot{y}^* = 0$ and the decoupling and linearizing control is given by

$$u = D^{-1}C\mathcal{L}^{-1}[(\Omega(\omega)\mathcal{L} + \mathcal{R})x - M_2 v_s]$$

with

$$D = C\mathcal{L}^{-1}M_1 = -\frac{L_{sr}}{L_s L_r - L_{sr}^2} I_2 < 0,$$

where negative definiteness stems from the fact that $L_s L_r > L_{sr}^2$. Substituting this control into the system equations, one gets the following dynamics

$$\dot{x} = Ax - \mathcal{L}^{-1}(I_4 - M_1 D^{-1} C\mathcal{L}^{-1})M_2 v_s$$

with

$$A = -\mathcal{L}^{-1}[\Omega(\omega)\mathcal{L} + \mathcal{R} - M_1 D^{-1} C\mathcal{L}^{-1}(\Omega(\omega)\mathcal{L} + \mathcal{R})].$$

Some lengthy, but straightforward, calculations yield

$$A = \begin{bmatrix} 0 & 0 \\ -\frac{1}{L_{sr}}(\omega_s L_s J_2 + R_s I_2) & -\omega_s J_2 \end{bmatrix}$$

which, interestingly, is a constant matrix independent of ω , with the forcing term matrix

$$\mathcal{L}^{-1}(I_4 - M_1 D^{-1} C \mathcal{L}^{-1}) M_2 = \begin{bmatrix} 0 \\ 0 \\ * \\ * \end{bmatrix}$$

where $*$ denotes some non-zero constants. From these calculations we see that the first two components of the vector x , that is i_s , remain constant. The remaining, i_r , dynamics consists of a linear oscillator (with eigenvalues at $\pm j\omega_s$) with a constant forcing input that depends on v_s . It is well-known that a linear oscillator is not bounded-input bounded-output stable hence unbounded trajectories of the forced system may appear upon change of the line voltage, which stymies the control of the system by direct inversion.

We should underscore that a similar result is obtained if we take as output the rotor current, instead of that of the stator [15].

4. Power Flow Strategy

The power management schedule is determined according to the following considerations. The general goal is to supply the required power to the load with a high-network power factor, i.e. $Q_n \sim 0$, where Q_n is the network reactive power. On the other hand, we will show that the DFIM has an optimal mechanical speed for which there is minimal power injection through the rotor. Combining these two factors suggests to consider the following three modes of operation:

- *Generator mode.* When the real power required by the local load is bigger than the maximum network power (say, P_n^M) we use the DFIM as a generator. In this case we fix the references for the network real and reactive powers as $P_n^* = P_n^M$ and $Q_n^* = 0$.
- *Storage (or motor) mode.* When the local load does not need all the network power and the mechanical speed is far from the optimal value the “unused” power network is employed to accelerate the flywheel. From the control point of view, this operation mode coincides with the *generator mode*, and thus we fix the same references – but now we want to extract the maximum power from the network to transfer it to the flywheel.
- *Stand-by mode.* Finally, when the local load does not need all the power network and the mechanical speed is near to the optimal one we just compensate for the flywheel friction losses by regulating the

Table 1. Control action table.

$P_n^* < P_1$	$ \omega - \omega_s \leq \epsilon$	Mode	Control	References
True	True	Generator	0	$P_n^* = P_n^M$ and $Q_n^* = 0$
True	False	Generator	0	$P_n^* = P_n^M$ and $Q_n^* = 0$
False	True	Stand-by	1	$Q_n^* = 0$ and $\omega^* = \omega_s$
False	False	Storage	0	$P_n^* = P_n^M$ and $Q_n^* = 0$

speed and the reactive power. Hence, we fix the reference for the mechanical speed at its minimum rotor losses value (to be defined later) and set $Q_n^* = 0$.

The operation modes boil down to two kinds of control actions (we call them 0 and 1) as expressed in Table 1, where P_1 is the load power and $\epsilon > 0$ is some small parameter.

To formulate mathematically the power flow strategy described above we need to express the various modes in terms of equilibrium points. In this way, the policy will be implemented transferring the system from one equilibrium point to another. Towards this end, we compute first the fixed points of our system (6), i.e. the values $z_e^* = \mathcal{L}i^*$, $z_m^* = J_m\omega^*$, v_r^* such that

$$[\mathcal{J}(z^*) - \mathcal{R}] \begin{bmatrix} i^* \\ \omega^* \end{bmatrix} + B_1 v_r^* + B_2 v_s = 0.$$

Explicit separation of the rows corresponding to the stator, rotor, network and mechanical equations yields the following system of equations:

$$\omega_s L_s J_2 i_s^* + \omega_s L_{sr} J_2 i_r^* + R_s I_2 i_s^* - v_s = 0 \quad (7)$$

$$(\omega_s - \omega^*) [L_{sr} J_2 i_s^* + L_r J_2 i_r^*] + R_r I_2 i_r^* - v_r^* = 0 \quad (8)$$

$$L_{sr} i_s^{*\top} J_2 i_r^* - B_r \omega^* = 0. \quad (9)$$

It is clear that – assuming no constraint on v_r – the key equations to be solved are (7) and (9).

As discussed above, a DFIM has an optimal mechanical speed for which there is minimal power injection through the rotor. Indeed, from (8) one immediately gets

$$P_r^* \triangleq i_r^{*\top} v_r^* = (\omega_s - \omega^*) L_{sr} i_r^{*\top} J_2 i_s^* + R_r |i_r^*|^2,$$

where $|\cdot|$ is the Euclidean norm. Further, using (9), we get

$$P_r^* = B_r \omega^* (\omega^* - \omega_s) + R_r |i_r^*|^2. \quad (10)$$

Although the ohmic term in (10) does depend also on ω , its contribution is small for the usual range of

parameter values, so $|P_r|$ is small near $\omega^* = \omega_s$. Another consideration that we make to justify our choice of “optimal” rotor speed, ω^* , concerns the reactive power supplied to the rotor – that we would like to minimize. It can be shown that

$$Q_r^* \triangleq i_r^{*\top} J_2 v_r^* = (\omega^* - \omega_s) f(Q_n, \omega^*),$$

where $f(\cdot, \cdot)$ is a bounded function of its arguments. Consequently, $Q_r^* = 0$ for $\omega^* = \omega_s$. Taking this into account, we will set the reference of the mechanical speed as $\omega^* = \omega_s$.

Let us explain now the calculations needed to determine the desired equilibria for the generating and stand-by modes. Assuming a sinusoidal steady-state regime, the network active and reactive powers are defined as follows:

$$P_n \triangleq i_n^\top v_s = V_0 i_{nd} \quad (11)$$

$$Q_n \triangleq i_n^\top J_2 v_s = V_0 i_{nq}, \quad (12)$$

where $i_n = [i_{nd}, i_{nq}]^\top$.

In generator (and storage) mode we fix $P_n^* = P_n^M$ and $Q_n^* = 0$, and thus immediately obtain from (11) and (12) that $i_n^* = [P_n^M/V_0, 0]^\top$. Next, from Eq. (1) and the measured i_i we obtain i_s^* which, upon replacement on (7) yields i_r^* . Then, ω^* is computed from Eq. (9), and finally v_r^* is obtained via (8).

For the stand-by mode we still set $Q_n^* = 0$, but now fix $\omega^* = \omega_s$. This is a more complicated scenario as we have to ensure the existence of i_s^* and i_r^* solutions for the nonlinear Eqs (7) and (9). First of all, multiplying Eq. (7) by $i_s^{*\top}$ and using Eq. (9) one gets

$$R_s |i_s^*|^2 - v_s^\top i_s^* + B_r \omega_s^2 = 0. \quad (13)$$

This is a quadratic equation in the two components of i_s^* . It may have an infinite number of solutions, a unique one, or no solution at all, depending on whether ω_s is smaller, equal or larger than $V_0/\sqrt{2}B_rR_s$, respectively. Since B_r is usually a small coefficient typically there will be an infinite number of i_s^* that solve the equation. We will choose then the one of minimum norm. Once we have fixed i_s^* we can proceed as in the generating mode to compute i_r^* and v_r^* .

Before closing this section we make the observation that, under the assumptions that the load can be modelled as a linear RL circuit and small friction coefficient, we can get a simple condition on the load parameters that ensure the existence of ω^* and P_n^* , with $Q_n^* = 0$. Indeed, taking a general RL-load

$$Z_1 = R_1 I_2 + \omega_s L_1 J_2,$$

replacing in Eq. (13), using Eq. (1), and the network power definitions (11) and (12) we obtain

$$(P_n^*)^2 - |v_s|^2 \left(\frac{2R_1}{|Z_1|^2} + \frac{1}{R_s} \right) P_n^* + \frac{|v_s|^4}{|z_1|^2} \left(1 + \frac{R_1}{R_s} + \frac{2\omega_s L_1 Q_n^*}{|v_s|^2} \right) - \frac{|v_s|^2 B_r \omega_s^2}{R_s} = 0.$$

In our case $Q_n^* = 0$ and considering $B_r = 0$ yields the quadratic equation

$$(P_n^*)^2 - |v_s|^2 \left(\frac{2R_1}{|Z_1|^2} + \frac{1}{R_s} \right) P_n^* + \frac{|v_s|^4}{|Z_1|^2} \left(1 + \frac{R_1}{R_s} \right) = 0.$$

It is easy to show that this equation has a positive real solution if and only if

$$R_s < \frac{R_1^2}{2\omega_s L_1} + \frac{\omega_s L_1}{2}, \quad (14)$$

and hence it always has a real solution for loads with sufficiently small inductance.

5. Controller Design

As mentioned in the Introduction section, to implement the proposed power flow strategy we design an IDA-PBC [10]. The central idea of this technique is to assign to the closed loop a desired energy function via the modification of the interconnection and dissipation matrices, still preserving the PCH structure. That is, the desired target dynamics is a PCH system of the form

$$\dot{z} = [\mathcal{J}_d(z) - \mathcal{R}_d(z)](\nabla H_d)^\top \quad (15)$$

where $H_d(z)$ is the new total energy and $\mathcal{J}_d(z) = -\mathcal{J}_d^\top(z)$, $\mathcal{R}_d(z) = \mathcal{R}_d^\top(z) > 0$, are the new interconnection and damping matrices, respectively. To achieve stabilization of the desired equilibrium point we impose

$$z^* = \arg \min H_d(z).$$

It is easy to see that the matching objective is achieved if and only if the following matching equation is satisfied

$$[\mathcal{J}_d(z) - \mathcal{R}_d(z)](\nabla H_a)^\top = -[\mathcal{J}_a(z) - \mathcal{R}_a(z)](\nabla H)^\top + B_1 v_r + B_2 v_s \quad (16)$$

where, for convenience, we have defined

$$\begin{aligned} H_d(z) &= H(z) + H_a(z), \mathcal{J}_d(z) = \mathcal{J}(z) + \mathcal{J}_a(z), \\ \mathcal{R}_d(z) &= \mathcal{R}(z) + \mathcal{R}_a(z). \end{aligned}$$

Notice that v_s is fixed, so the only available control is v_r .

The standard way to solve Eq. (16) is to fix the matrices $\mathcal{J}_a(z)$ and $\mathcal{R}_a(z)$ – hence the name IDA – and then solve the matching equation, which is now a PDE in $H_a(z)$. In general, solving PDEs is a complicated task. Fortunately, the special structure of our system allows us, in the spirit of Refs [5,12], to fix $H_d(z)$ – transforming (16) into a purely algebraic equation – and then solve it for $\mathcal{J}_a(z)$ and $\mathcal{R}_a(z)$.

5.1. Solving the Matching Equation

Following the strategy outlined above to solve the matching Eq. (16), we choose a desired quadratic total energy

$$H_d(z) = \frac{1}{2}(z_e - z_e^*)^\top \mathcal{L}^{-1}(z_e - z_e^*) + \frac{1}{2J_m}(z_m - z_m^*)^2,$$

which clearly has a global minimum at the desired fixed point. This implies

$$\begin{aligned} H_a(z) &= H_d(z) - H(z) \\ &= -z_e^{*\top} \mathcal{L}^{-1} z_e - \frac{1}{J_m} z_m^* z_m + \frac{1}{2} z_e^{*\top} \mathcal{L}^{-1} z_e^* + \frac{1}{2J_m} z_m^{*2}. \end{aligned}$$

Note that

$$(\nabla H_a)^\top = \begin{bmatrix} -i^* \\ -\omega^* \end{bmatrix}.$$

Using this relation, (16) becomes

$$\begin{aligned} [\mathcal{J}_d(z) - \mathcal{R}_d(z)] \begin{bmatrix} i^* \\ \omega^* \end{bmatrix} &= [\mathcal{J}_a(z) - \mathcal{R}_a(z)] \begin{bmatrix} i \\ \omega \end{bmatrix} \\ &\quad - B_1 v_r - B_2 v_s. \end{aligned} \quad (17)$$

The control action appears on the third and fourth rows, which suggests the choice

$$\begin{aligned} \mathcal{J}_a(z) &= \begin{bmatrix} O_2 & O_2 & O_{2 \times 1} \\ O_2 & O_2 & -\mathcal{J}_{rm}(z) \\ O_{1 \times 2} & \mathcal{J}_{rm}^\top(z) & 0 \end{bmatrix}, \\ \mathcal{R}_a &= \begin{bmatrix} O_2 & O_2 & O_{2 \times 1} \\ O_2 & rI_2 & O_{2 \times 1} \\ O_{1 \times 2} & O_{1 \times 2} & 0 \end{bmatrix} \end{aligned} \quad (18)$$

where $\mathcal{J}_{rm}(z) \in \mathbb{R}^{2 \times 1}$ is to be determined, and we have injected an additional resistor $r > 0$ for the rotor currents to damp the transient oscillations.

Substituting (18) in (17) and using the fixed-point equations, one gets, after some algebra,

$$\begin{aligned} \mathcal{J}_{rm}^\top(z) &= L_{sr} \frac{(i_r - i_r^*)^\top}{|i_r - i_r^*|^2} (i_s - i_s^*)^\top J_2 i_r^*, \\ v_r &= v_r^* - (\omega - \omega^*) (L_r J_2 i_r^* + \mathcal{J}_{rm}(z)) \\ &\quad - L_{sr} \omega^* J_2 (i_s - i_s^*) - r I_2 (i_r - i_r^*). \end{aligned}$$

Unfortunately, the control is singular at the fixed point. Although from a numerical point of view we could implement it by introducing a regularization parameter, we are going to show below that it is possible to get rid of the singularity by adding a variable damping which turns out to decouple the mechanical and electrical subsystems.

5.2. Subsystem Decoupling via State-Dependent Damping

We keep the same $H_d(z)$ and $\mathcal{J}_d(z)$ as before, but instead of the constant \mathcal{R}_a given in (18) we introduce a state-dependent damping matrix

$$\mathcal{R}_a(z) = \begin{bmatrix} O_2 & O_2 & O_{2 \times 1} \\ O_2 & rI_2 & O_{2 \times 1} \\ O_{1 \times 2} & O_{1 \times 2} & \xi(z) \end{bmatrix},$$

where we set

$$\xi(z) = \frac{\tau_e^* - \tau_e(z)}{\omega - \omega^*}$$

with τ_e the electrical torque

$$\tau_e = L_{sr} i_s^\top J_2 i_r$$

and $\tau_e^* = B_r \omega^*$ its fixed point value. Notice that, when substituted into the closed-loop Hamiltonian equations, $\xi(z)$ is multiplied by $\omega - \omega^*$ and hence no singularity is introduced.

Since we have only changed the mechanical part of (17), only the value for $\mathcal{J}_{rm}(z)$ is changed while the expression for v_r in terms of $\mathcal{J}_{rm}(z)$ remains the same. After some algebra and using the fixed point equations, we get

$$\mathcal{J}_{rm}(z) = L_{sr} J_2 i_s.$$

The closed loop dynamical system is still of the form (15) with

$$\mathcal{J}_d(z) = \begin{bmatrix} -\omega_s L_s J_2 & -\omega_s L_{sr} J_2 & O_{2 \times 1} \\ -\omega_s L_{sr} J_2 & -(\omega_s - \omega) L_r J_2 & O_{2 \times 1} \\ O_{1 \times 2} & O_{1 \times 2} & 0 \end{bmatrix},$$

$$\mathcal{R}_d(z) = \begin{bmatrix} R_s I_2 & O_2 & O_{2 \times 1} \\ O_2 & (R_r + r) I_2 & O_{2 \times 1} \\ O_{1 \times 2} & O_{1 \times 2} & B_r + \xi(z) \end{bmatrix}.$$

We underscore the fact that the state-dependent ‘‘damping’’ is an artifice to decouple the electrical and mechanical parts in the closed-loop interconnection and dissipation matrices – and the proposed control is shaping only the electrical dynamics.

5.3. Main Stability Result

Owing to the fact that we cannot show that $B_r + \xi(z) \geq 0$, we cannot apply the standard stability analysis for PCH systems [16]. However, the overall system has a nice cascaded structure, with the electrical part a bona fide PCH subsystem with well-defined dissipation. (This situation is similar to the Nested PBC proposed in Chapter 8 of Ref. [9].) Asymptotic stability of the overall system follows from well-known properties of cascaded systems [14]. For the sake of completeness we give the specific result required in our example in the form of a lemma in the Appendix section.

We are in position to present the following:

Proposition 1. Consider the DFIM-based system (6) in closed-loop with the static state-feedback control

$$v_r = v_r^* - (\omega - \omega^*)(L_r J_2 \dot{i}_r^* + L_{sr} J_2 \dot{i}_s) - L_{sr} \omega^* J_2 (i_s - i_s^*) - r I_2 (i_r - i_r^*) \quad (19)$$

where

$$v_r^* = (\omega_s - \omega^*)[L_{sr} J_2 \dot{i}_s^* + L_r J_2 \dot{i}_r^*] + R_r I_2 \dot{i}_r^*$$

and (i_s^*, i_r^*, ω^*) correspond to desired equilibria. Assume the motor friction coefficient B_m is sufficiently small to ensure the solution of the equilibrium equations (7) and (9). Then, each operating mode of the proposed power flow policy is globally convergent.

Proof. Energy shaping of the electrical subsystem ensures that

$$\dot{H}_{de} \leq -\min\{R_s, R_r + r\} |z_e - z_e^*|^2,$$

where $H_{de} \triangleq \frac{1}{2} (z_e - z_e^*)^\top \mathcal{L}^{-1} (z_e - z_e^*)$. Consequently, $z_e \rightarrow z_e^*$ exponentially fast. The proof follows

immediately checking that the conditions of Lemma 1 in Appendix A hold. To do that, we identify x_1 with the electric variables and x_2 with the mechanical variables. The electric subsystem has (i_s^*, i_r^*) as a global asymptotically stable fixed point for any function $\omega(t)$. Hence, all trajectories of the closed-loop dynamics asymptotically converge to the equilibrium point (i_s^*, i_r^*, ω^*) . \square

6. Simulations

In this section we implement a numerical simulation of the IDA-PBC developed in the previous sections. We use the following parameters (in SI units): $L_{sr} = 0.041$, $L_s = L_r = 0.041961$, $J_m = 5.001$, $R_s = 0.087$, $R_r = 0.0228$, $B_r = 0.005$.

We have simulated two varying loads, one resistive and the other resistive-inductive.⁵ The resistive load is initially $R_l = 1000$, changes ramp-wise to $R_l = 5$ at $t = 1$ in 0.2 s and returns to $R_l = 1000$ at $t = 1.8$ also in 0.2 s. The same envelope (shifted 5 s forward) is used for the second load, with values $R_l = 1000$, $L_l = 0.1$ and $R_l = 5$, $L_l = 0.1$. The voltage source is, in dq coordinates, $v_s = (380, 0)$ and $\omega_s = 2\pi \cdot 50$. The simulation has been performed using the 20-sim [1] modeling and simulation software.

For the purposes of testing the controller, we have set a maximum power network $P_n = 10000$. The damping parameter is fixed at $r = 25$. A hysteresis filter is used to prevent chattering around $\omega = \omega_s$.

Figures 3–5 show the behavior for a purely resistive load for $t \in [0, 5]$. Note that, in Fig. 3, P_n tends to its maximum value even if the load demand (P_l) is higher. After the load demand returns to its initial value, P_n is kept at its peak value to accelerate the flywheel, until the later reaches the optimum speed. The evolution of ω during this sequence is also shown in Fig. 4; the minimum attained represents 96.2% of the optimal speed ω_s . Figure 5 shows the a -phase network voltage v_{sa} and current i_{na} , which have the same angle.

Figures 6–8 correspond to the varying RL load for $t \in [5, 10]$. Figure 6 shows the a -phase network voltage (v_{sa}) and network and load currents (i_{na} , i_{la}), where, although i_{la} is not in phase with v_{sa} , the controller is able to keep v_{sa} and i_{na} nearly in phase, so the actual reactive power Q_n remains close to zero. Also, as seen in Fig. 7, the minimum mechanical speed is 97.8% of the optimal value, while the goal of the maximal power from the network is also achieved, Fig. 8.

⁵Although the scenario of an RL load is not contemplated in our analysis, we have added these simulations as a robustness test.

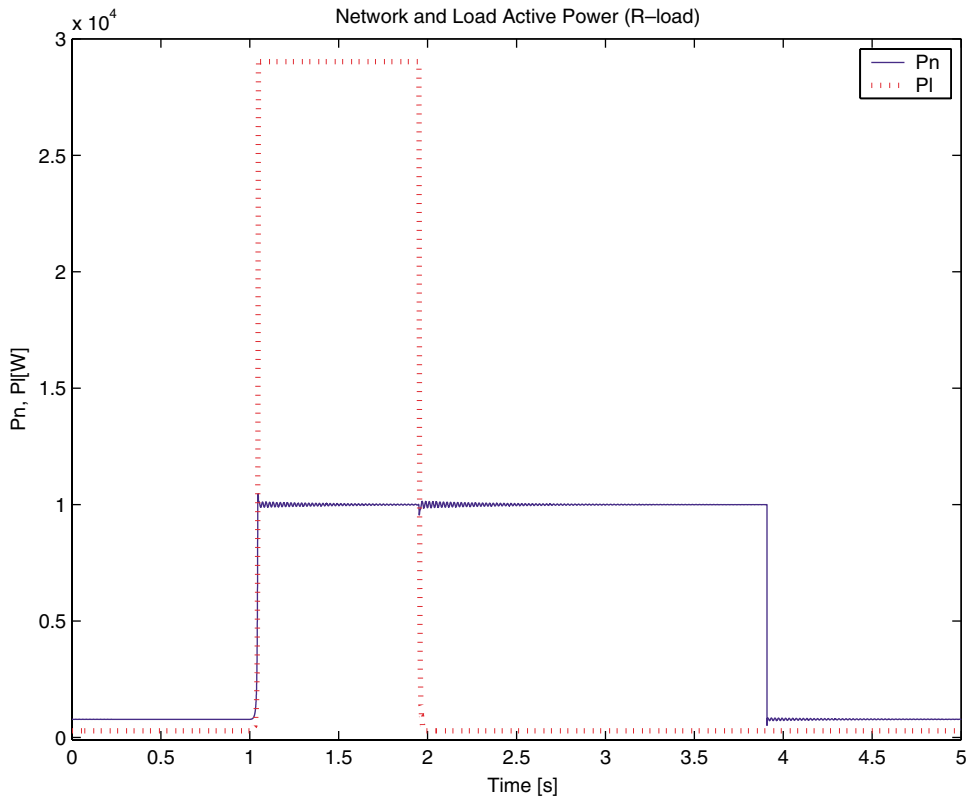


Fig. 3. Network and load active powers (P_n , P_l) for a resistive load.

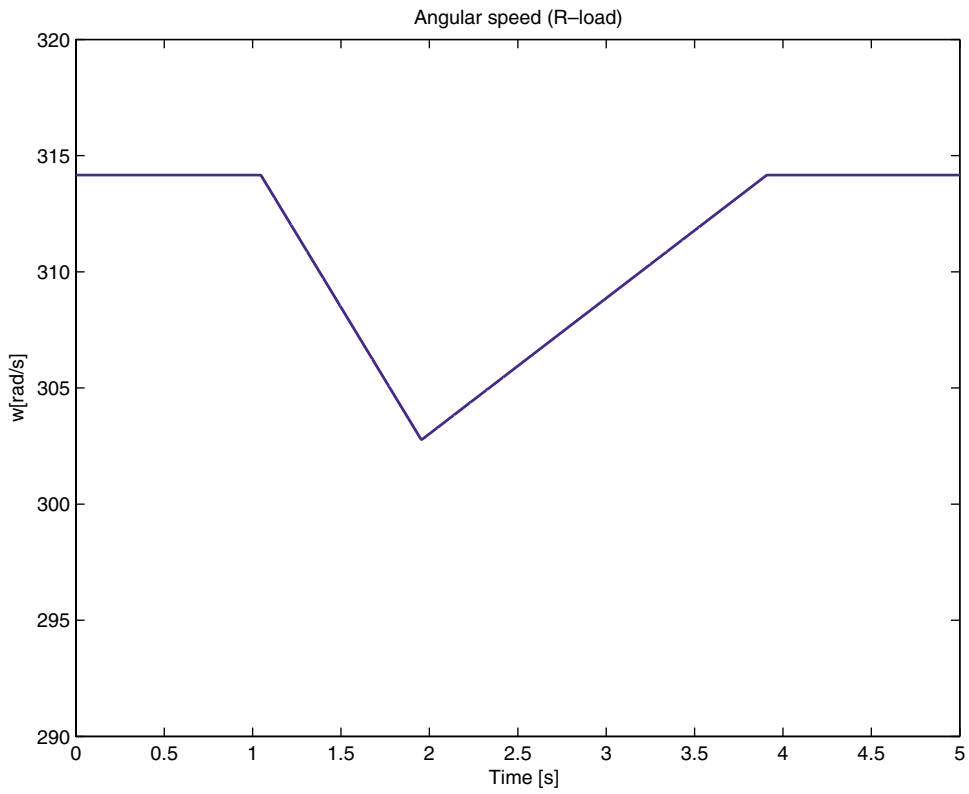


Fig. 4. Angular speed (ω) for a resistive load.

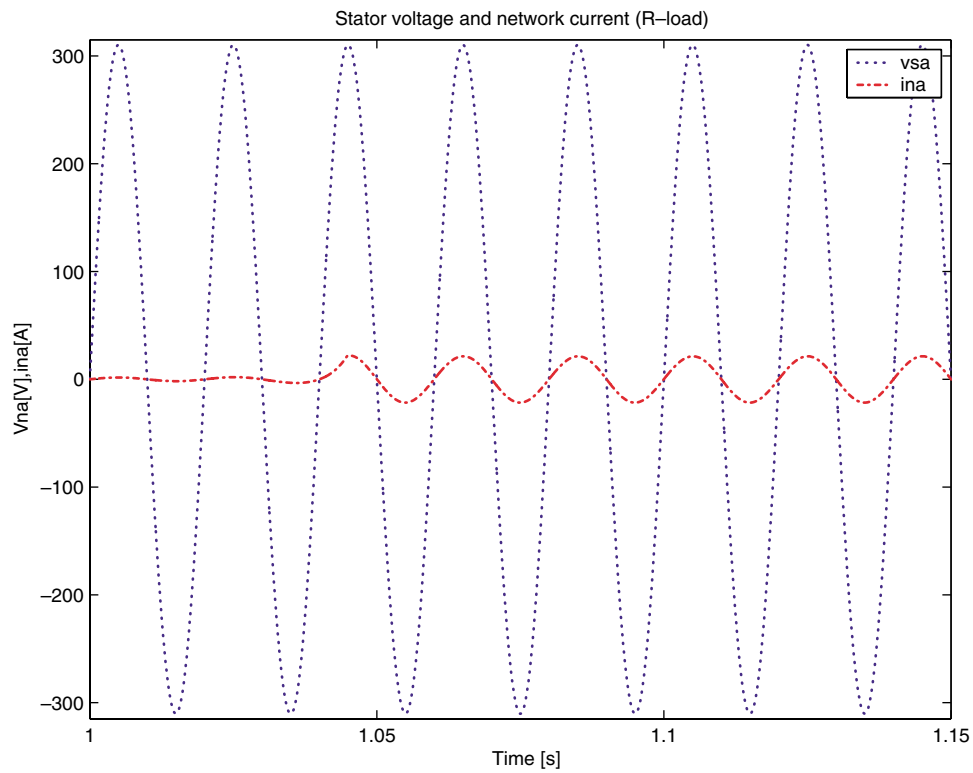


Fig. 5. Network voltage and current (v_{sa} , i_{na}) for a resistive load.

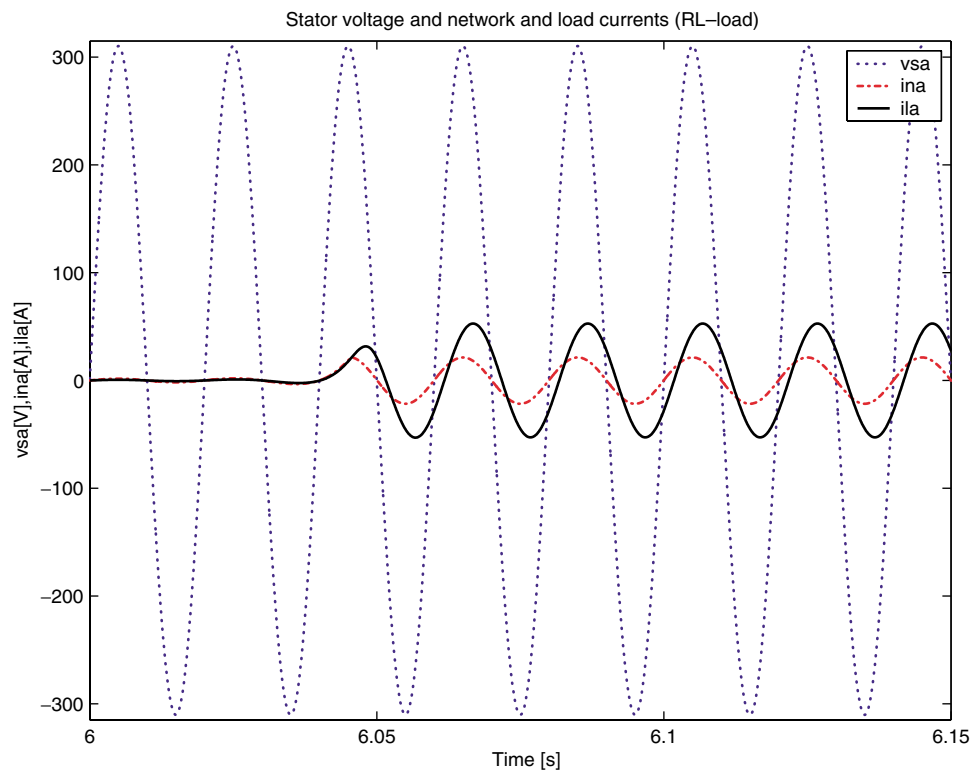


Fig. 6. Network voltage (v_{sa}) and network and load currents (i_{na} , i_{la}) for an RL load.

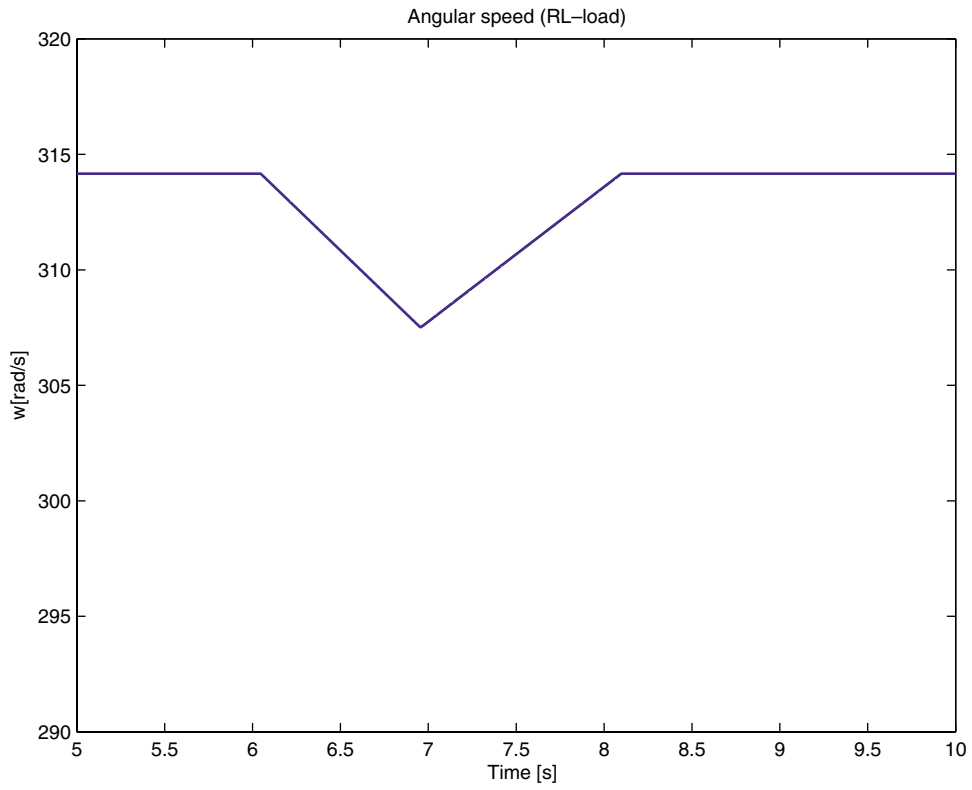


Fig. 7. Angular speed (ω) for an RL load.

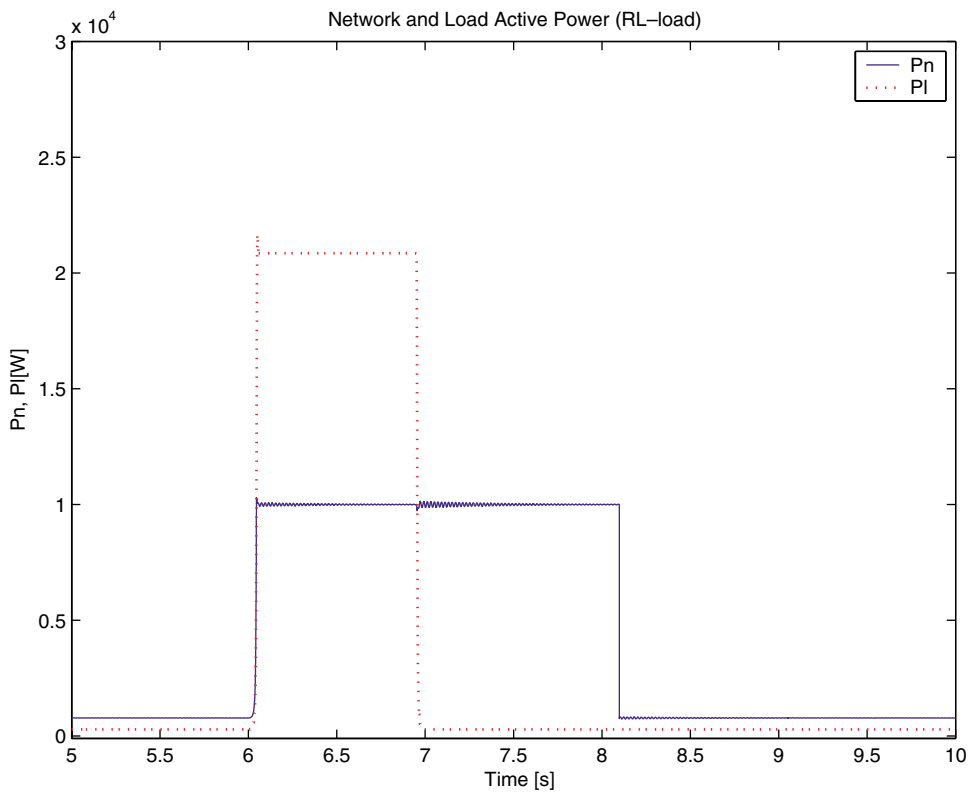


Fig. 8. Network and load active powers (P_n , P_l) for an RL load.

7. Conclusions and Outlook

IDA-PBC techniques have been applied to the control of a doubly-fed induction machine in order to manage the power flow between a mechanical source (flywheel) and a varying local load, under limited grid power conditions. We have been able to solve the IDA-PBC equations by assigning the desired Hamiltonian and introducing a variable damping to eliminate the resulting singularity. The controller obtained is globally convergent and decouples the mechanical and electrical subsystems in the interconnection matrix.

The system not only provides the active power required by the load, but also at the same time compensates the reactive power, so that the power grid sees the load+machine system as a pure resistive load, even for varying inductive local loads. There is no actual restriction about the kind of local load, as long as its parameters allow the assignment of equilibrium points.

We have established the stability of the equilibrium points corresponding to the three operating modes described in Table 1. However, stability cannot be ensured, without further analysis, when the power flow strategy that switches the operating modes is in place. If the switching is replaced by a smooth, sufficiently slow, transition from one operating point to the other we can invoke total stability arguments to prove that stability is preserved under some additional uniformity assumptions. Completing this analysis is the subject of on-going research.

Currently we are working on the experimental validation of the proposed controller, the implementation of the controller through a power converter connected also to the grid and the introduction of a grid model instead of the ideal bus considered in this paper.

References

1. *20sim* modeling and simulation software. Available on www.20sim.com
2. Akagi H, Sato H. Control and performance of a doubly-fed induction machine intended for a flywheel energy storage system. *IEEE Trans Power Elect* 2002; 17: 109–116
3. Caratozzolo P. Nonlinear control strategies of an isolated motion system with a double-fed induction generator. PhD Thesis, Universitat Politècnica de Catalunya, 2003
4. Dalsmo M, van der Schaft A. On representations and integrability of mathematical structures in energy-conserving physical systems. *SIAM J Control Optim* 1998; 37: 54–91

5. Fujimoto K, Sugie T. Canonical transformations and stabilization of generalized Hamiltonian systems. *Syst Control Lett* 2001; 42(3): 217–227
6. Krause PC. *Analysis of electric machinery*. McGraw-Hill, 1986
7. Kugi A. *Non-linear control based on physical models*. Springer, 2001
8. Leonhard W. *Control of electric drives*. Springer, 1995
9. Ortega R, Loria A, Nicklasson PJ, Sira-Ramirez H. *Passivity-based control of Euler-Lagrange systems*. Communications and Control Engineering. Springer-Verlag Berlin, Germany, 1998
10. Ortega R, van der Schaft A, Maschke B, Escobar G. Interconnection and damping assignment passivity-based control of port-controlled Hamiltonian systems. *Automatica* 2000; 38: 585–596
11. Peña R, Clare JC, Asher GM. Doubly fed induction generator using back-to-back PWM converters and its application to variable speed wind-energy generation. *IEE Proc Electric Power Appl* 1996; 143: 231–241
12. Rodríguez H, Ortega R. Stabilization of electromechanical systems via interconnection and damping assignment. *Int J Robust Nonlinear Control* 2003; 13: 1095–1111
13. Sillig JG, Polinder H, Kling WL. Dynamic modeling of a wind turbine with doubly fed induction generator. In: *Proceedings of the IEEE Power Engineering Society Summer Meeting*, pp 644–649, 2001
14. Sontag ED. On stability of perturbed asymptotically stable systems. *IEEE Trans Autom Control* 2003; 48(2): 313–314
15. Peresada S, Tilli A, Tonielli A. Power control of a doubly fed induction machine via output feedback. *Control Eng Practice* 2004; 12: 41–57
16. van der Schaft A. *L₂ gain and passivity techniques in nonlinear control*. 2nd edn. Springer, 2000

Appendix A

Lemma 1. Let us consider a system of the form

$$\begin{aligned}\dot{x}_1 &= f_1(x_1, x_2), \\ \dot{x}_2 &= -Bx_2 + h(x_1),\end{aligned}\tag{20}$$

where $x_1 \in \mathbb{R}^n$, $x_2 \in \mathbb{R}$, $B > 0$ and h is a continuous function. Assume that the system has fixed points x_1^* , x_2^* , and $\lim_{t \rightarrow +\infty} x_1(t) = x_1^*$ for any $x_2(t)$. Then $\lim_{t \rightarrow +\infty} x_2(t) = x_2^*$.

Proof. Let $(\sigma_1(t), \sigma_2(t))$ be a given solution to (20). Since $\lim_{t \rightarrow +\infty} \sigma_1(t) = x_1^*$ it follows that $\sigma_1(t)$ is bounded and so is $h(\sigma_1(t))$. Since $Bx_2^* = h(x_1^*)$, it follows that $\forall \epsilon > 0$ there exists $T > 0$, which may depend on $\sigma_1(t)$ and $\sigma_2(t)$, such that if $t > T$ then $|h(\sigma_1(t)) - Bx_2^*| < \epsilon \frac{B}{2}$. Using

$$1 = e^{-Bt} + B \int_0^t e^{-B(t-\tau)} d\tau$$

it is immediate to write,

$$\begin{aligned}
\sigma_2(t) - x_2^* &= e^{-Bt}(x_2(0) - x_2^*) \\
&+ \int_0^t e^{-B(t-\tau)}(h(\sigma_1(\tau)) - Bx_2^*) d\tau \\
&= e^{-Bt}(x_2(0) - x_2^*) \\
&+ \int_0^T e^{-B(t-\tau)}(h(\sigma_1(\tau)) - Bx_2^*) d\tau \\
&+ \int_T^t e^{-B(t-\tau)}(h(\sigma_1(\tau)) - Bx_2^*) d\tau
\end{aligned}$$

where $t > T$ has been assumed. There exists $\tilde{T} > 0$ such that if $t > \tilde{T}$ then

$$e^{-Bt} \left(x_2(0) - x_2^* + \int_0^T e^{B\tau} (h(\sigma_1(\tau)) - Bx_2^*) d\tau \right) > \frac{\epsilon}{2},$$

where the boundedness of h has been used. Furthermore

$$\begin{aligned}
&\left| \int_T^t e^{-B(t-\tau)} (h(\sigma_1(\tau)) - Bx_2^*) d\tau \right| \\
&< \int_T^t e^{-B(t-\tau)} \epsilon \frac{B}{2} d\tau \\
&= \frac{\epsilon}{2} (1 - e^{-B(t-T)}) < \frac{\epsilon}{2}.
\end{aligned}$$

Finally, taking $t > \max\{T, \tilde{T}\}$, one gets $|\sigma_2(t) - x_2^*| < \epsilon$. This ends the proof. \square